Energy Saving Theoretical Principles and Their Technological Implementation in High-Temperature Production of Building, Household and Technical Ceramics

Olena Yu. Fedorenko*, Yaroslav M. Pitak, Serhii V. Kartyshev, Petro Kapustenko

National Technological University "Kharkiv Polytechnic Institute", Department of Ceramics, Refractories, Glass and Enamel Technologies
fedorenko_e@ukr.net

The priority areas for the development of different purposes ceramics technology are the energy-saving technologies creation and the reduction of production energy costs. The main efforts should be directed to the implementation of energy-saving reserves at the firing stage of products as the most energy-intensive technological operation. The necessity of temperature reduction and the firing time shortening requires special attention to the ceramic masses and glazes prescripts, designed to ensure high-quality products under energy-saving firing conditions. This paper considers the new approach for low-temperature masses and frit-free glaze development and presents an algorithm for composition designing in the production of building, technical and household ceramics. Examples of the original and low-cost method used for the energy-saving reserves implementation in porcelain slabs, electrical, sanitary and tableware porcelain production are given. The effectiveness of the proposed method was experimentally confirmed. Its use made it possible to reduce the firing temperature of products by 100-150 °C, significantly shorten the production cycle and, as a result, reduce energy costs by 15-20 %.

1. Introduction

The modern ceramics industry is one of the most energy-intensive: approximately 28 % of consumed energy is spent on production (Giacone and Mancò, 2012). In this regard, ceramic enterprises faced problems associated with the low energy efficiency of technological processes. Firing is the most important technological stage in ceramic materials production, providing the products with the necessary technical and aesthetic properties. At the same time, firing is the most energy-intensive technological operation, characterised by a large amount of waste heat (up to 80–95 %). The share of firing in the structure of total costs for the production of the main ceramics types ranges from 50 % for porcelain tiles (Almeida et al., 2016) to 90 % (Cuviella-Suárez et al., 2019) for electro-porcelain products (Castro Oliveira et al., 2020).

For ceramic products of various purposes, firing is carried out in continuous furnaces operating on natural gas. Gas-fired kilns are not environmentally friendly: continuous burning of natural gas for firing results in significant CO_2 emissions. Nevertheless, such furnaces are widely used now throughout the world. More than 8,000 furnaces operate in ceramic tile production enterprises alone (Monfort et al., 2010). Considering the average energy consumption of a kiln, the annual global energy consumption for firing ceramic tiles is estimated at approximately $1.82 \cdot 10^5$ GWh (Caglayan and Caliskan, 2019). According to most researchers, this is due to the high temperature (1,200-1,400 °C) and long firing time, as well as large heat losses to the environment.

The exergy analysis of the furnace operation, performed based on experimentally obtained thermographic data, confirmed the low furnace energy efficiency (Ferrer et al., 2019). It also made it possible to determine the causes of inefficient energy use, as well as the losses scales: it has been established that only 10 % of the supplied exergy is spent on physical and chemical transformations during the phase composition and structure of porcelain stoneware formation. Detailed exergy analysis of the kiln operation made it possible to identify and quantify the main irreversibility sources: natural gas combustion, heat transfer during fired tiles cooling and heat

transfer through the kiln surfaces. The research results indicate the possibility of an energy efficiency increase of a roller kiln due to the waste heat recovery of more than 61 %.

Summarising the results of studies (Mezquita et al., 2014), it can be concluded that the energy efficiency of roller kilns can be improved through the introduction of exhaust gas heat recovery systems using heat exchangers, using burners operating at lower air pressure, heating the air supplied for combustion; improve the furnace thermal insulation. However, the implementation of these measures requires significant economic investment.

Kapustenko et al. (2020) point out the heat recovery feasibility due to heat exchangers used for the energy efficiency of furnace equipment increasing in ceramics production. Delpech et al. (2018) also discuss the heat exchangers' efficiency and identify the potential recovery of thermal energy (863 MWh). Indicated the possibility of reducing gas consumption (approximately 110,600 m^3), which would save more than 22,000 € annually and eliminate emissions of 164 t CO_2.

Analysis of the energy saving issue in ceramic tiles production showed a great interest in the firing energy efficiency. Most of the works presented by Mullinger and Jenkins (2008), are focused on the technical and energy issue side, in particular on furnaces operation modernisation and firing modes optimisation. However, they are not ascertaining the possibility of technological energy-saving reserves, which implementation does not require large production costs. At the same time, the use of low-temperature masses and glazes can reduce the temperature and shorten firing time while maintaining high product quality. According to (Song, 2018), reducing the temperature and duration of firing products in the production of ceramic tiles will reduce fuel consumption by ~30 % and significantly reduce CO_2 emissions.

The objective of this paper is to present the developed methodology of masses and glaze creation for ceramic product production with various functional purposes under energy-saving firing conditions.

2. Methodology for masses and glazes compositions designing

A composition choice for the ceramic material and glasses with a given phase composition is based on state diagrams of phase-forming oxide systems. These diagrams are obtained using factorial experiments methods with sensitivity analysis by regression and uncertainty estimation with triple measurements at experimental points. The sub-solidus analysis of systems allows: (a) determine the conditions of the crystalline phase that form a given phase composition of the material; (b) predict the formation conditions of the liquid phase during material heat treatment to evaluate the dynamics of its accumulation under specified temperature conditions; (c) estimate the phase transformation temperatures correspondence to the technological process conditions.

The proposed method of ceramic masses and glazes designed for obtaining various purposes of aluminosilicate ceramics consists in predicting the behaviour of real poly-component objects by modelling their melting and phase formation. It is using a set of state diagrams of elementary ternary subsystems of a basic multi-component system. The determination of the materials' phase composition at given firing temperatures is carried out by graph-analytical calculations using the lever rule. The calculation algorithm involves the following steps:

1*) Determination of the main phase-forming oxides based on the material chemical composition data.*
Phase-forming oxides are oxides, the amount of which in the chemical material composition exceeds 1 wt. %. If the material contains more than three phase-forming oxides, two or three subsystems should be considered.

2*) Reducing a real multicomponent material composition to basic systems of phase-forming oxides.*
The chemical composition of the ceramic material or glaze should be reduced to one or more three-component model compositions in accordance with the selected subsystems of the phase-forming oxides. After plotting the figurative point of the model oxide composition of the developed material on the state diagram of the selected oxide subsystems, graph-analytical calculations are carried out.

3) Melting diagrams construction of the model's compositions using three-component state diagrams of phase-forming oxides ($Na_2O–Al_2O_3–SiO_2$, $K_2O–Al_2O_3–SiO_2$; $CaO–Al_2O_3–SiO_2$ etc.).
Melting diagrams characterise the material state dependence on the firing temperature. To build them, it is necessary to use state diagrams on which isotherms are plotted. To determine the phase number, the well-known lever rule is used. If a system temperature parameter change causes the decomposition of one phase into two others, then the quantitative ratio of the newly formed phases is inversely proportional to the lengths of segments from the initial phase composition point to the composition points of the newly formed phases.

4) Graphical determination of the temperature of the beginning of melting and the temperature of the liquidus according to the melting diagrams obtained using three-component diagrams Eqs(1) and (2).

$$\left(T_{mb}\right)_i - \left(T_{mb}\right)N - A - S; \left(T_{mb}\right)K - A - S; \left(T_{mb}\right)C - A - S \tag{1}$$

$$\left(T_{liqv}\right)_i - \left(T_{liqv}\right)N - A - S; \left(T_{liqv}\right)K - A - S; \left(T_{liqv}\right)C - A - S \tag{2}$$

Here i is the component: Na_2O, K_2O, CaO.

5) Graphical determination of the type and number of solid phases that exist at a given firing temperature (T_S) according to melting diagrams – Eqs(3) and (4):

$$\left(Q_{liqv}^{Ts}\right)_i - \left(Q_{liqv}^{Ts}\right)N - A - S; \left(Q_{liqv}^{Ts}\right)K - A - S; \left(Q_{liqv}^{Ts}\right)C - A - S \tag{3}$$

$$\left(Qz_{sol}^{Ts}\right)_i - \left(Qz_{sol}^{Ts}\right)N - A - S; \left(Qz_{sol}^{Ts}\right)K - A - S; \left(Qz_{sol}^{Ts}\right)C - A - S \tag{4}$$

Here i is the oxide Na_2O, K_2O, CaO; z – solid phases existing at a given firing temperature.

6) Obtained data refinement is carried out considering the ratios of the components Na_2O, K_2O, CaO.

If the calculations were performed in two or more oxides systems it is necessary to refine data considering the correction factors that determine the percentage of each oxide (K_2O, Na_2O or CaO) in their total amount by Eq(5) – Eq(8):

$$\overline{T}_{mb} = \frac{\sum_{i=1}^{j} M_i \cdot (T_{mb})_i}{\sum_{i=1}^{j} M_i} \tag{5}$$

$$\overline{T}_{liqv} = \frac{\sum_{i=1}^{j} M_i \cdot (T_{liqv})_i}{\sum_{i=1}^{j} M_i} \tag{6}$$

$$\overline{Q}_{liqv}^{Ts} = \frac{\sum_{i=1}^{j} M_i \cdot (Q_{liqv}^{Ts})_i}{\sum_{i=1}^{j} M_i} \tag{7}$$

$$\overline{Q}z_{sol}^{Ts} = \frac{\sum_{i=1}^{j} M_i \cdot (Qz_{sol}^{Ts})_i}{\sum_{i=1}^{j} M_i} \tag{8}$$

Here M_i is the oxides content (Na_2O, K_2O or CaO) in the material, mol. %.

7) Determination of the oxides content bound in solid phases, is carried out according to the melting diagram taking into account the quantitative and qualitative solid phase composition at a given temperature. Clarification of the obtained data is accounting for the real oxides ratio K_2O, Na_2O, CaO by Eqs(9)-(10):

$$Pn_{sol}^{Ts} = \sum_{z=1}^{m} P_{sol}^{Ts} \tag{9}$$

$$\overline{P}n_{sol}^{Ts} = \frac{\sum_{z=1}^{m} M_i \cdot (Pn_{sol}^{Ts})}{\sum_{i=1}^{j} M_i} \tag{10}$$

Here M_i is the content of an oxide from the series Na_2O, K_2O, CaO, mol. %; m are oxides included in the solid phase composition; z – are solid phases present in the material at a given temperature T_S;

8) Calculation of the melt chemical composition at a given temperature (T_s) during the product firing by Eq(11)

$$Pn_{liqv}^{Ts} - Pn_{sol}^{Ts} \tag{11}$$

Here Pn_{liqv}^{Ts} is the content of the n-oxide (wt.%) in the melt, which is formed at a given heat treatment temperature T_S; Pn_{sol}^{Ts} is the content of the n-oxide (wt.%), which is in the solid phase at a given heat treatment temperature T_S; Pn_{inc} is the content of the n-oxide in the initial material composition, wt.%;

Such considerations are quite logical since when the firing temperature conditions change, the melt composition changes too due to the solid phase's dissolution or the new phase's formations, which affects its properties. The chemical composition of the melt calculated in this way must be brought to 100 % before further calculations of its properties are carried out.

9) Calculation of the melt properties that determine the ceramic products' sintering intensity (viscosity, surface tension, ability to dissolve the solid phase, etc.).

The calculation of the melt properties is carried out using mathematical models that describe the dependencies "composition-property" considering the ceramic materials' firing conditions. The highest convergence of experimental and calculated results is observed when using statistical models of Fludgel (2007) and also Goleus and Saley (2015) (the maximum relative calculations errors do not exceed 3 % and 5 %). The second method allows calculating the boron-including alkaline aluminosilicate melts properties containing a significant amount of alkaline earth metals oxides. In the case of using this technique for glass-crystal glazes compositions

designing, the melt composition data make it possible to obtain information on the melt depolymerisation degree, its crystallisation ability, as well as structural features (coordination state of boron and aluminium ions), which determine the formation of the crystalline phase.

3. Results and discussion

From the point of energy saving view in fine ceramics production, it is important to ensure the completion of the sintering and phase formation processes at low temperatures in the shortest possible time. The $Na_2O–K_2O–Al_2O_3–SiO_2$ system is the basis for the many types of densely sintered ceramics creation, in particular, porcelain tiles and porcelain products for various purposes. This system in the subsolidus region is divided into 68 elementary tetrahedrons (Figure 1a). Studies of the subsolidus state of the $Na_2O–K_2O–Al_2O_3–SiO_2$ system have established that the composition of the NAS_6-KAS_6-A_3S_2-S tetrahedron is the most promising for the composition's design suitable for the fine ceramic products manufacture under energy-saving firing conditions (Figure 1b). This tetrahedron contains mullite (A_3S_2), which improves the ceramics' mechanical, chemical and dielectric properties. It is characterised by a large elementary volume and numerous low-temperature eutectics: *binary* - between albite NAS_6 and leucite KAS_4 (1,075 °C), between leucite KAS_4 and quartz (1,150 °C), between orthoclase KAS_6 and quartz (990 °C), between albite NAS_6 and quartz (1,062 °C); *ternary* - between leucite KAS_4, orthoclase KAS_6 and mullite A_3S_2 (1,140 °C), between mullite A_3S_2, albite NAS_6 and quartz (1,050 °C), between orthoclase KAS_6, mullite A_3S_2 and quartz (985 °C); *four-component* -: between mullite A_3S_2, albite NAS_6, orthoclase KAS_6 and quartz (1,039 °C).
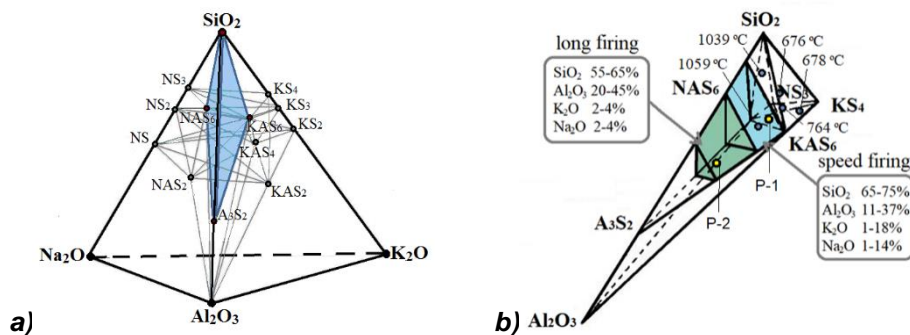

Figure 1: Subsolidus structure of the $Na_2O–K_2O–Al_2O_3–SiO_2$ system (a) and the region of oxide compositions for obtaining products by high-speed and long-term firing modes (b)

This allows to assume that when the masses are fired at relatively low temperatures (1,150-1,200) °C, a liquid phase sufficient amount for intensive sintering will be formed. The NAS_6-KAS_6-A_3S_2-S tetrahedron areas that are the most promising for obtaining fine ceramic materials with a reduced firing temperature in conditions of high-speed and long-term firing were determined (Figure 1b). The example of sintering and phase formation conditions determined during the firing of two different masses is shown in Figure 2. The composition P-1 was chosen in the widest part of the NAS_6-KAS_6-A_3S_2-S tetrahedron near the eutectic. When the mass is fired at a temperature of 1,150-1,200 °C, a large melt amount formation is required for sintering under high-speed firing conditions. The P-2 composition is located in the central part of the tetrahedron and belongs to the crystallisation region of the mullite phase. Such a choice should increase the mullite phase amount to ensure the required high mechanical and electrical strength of electrical porcelain. Calculations showed that when the firing temperature increased to 1,250 °C, the liquid phase amount in the firing products of mass P-1 grew to 55 %. Sufficiently slow melt formation makes it possible to exclude its avalanche-like accumulation and resulting high-temperature deformation of products. During the firing of the mass P-2 in the temperature range 1,200-1,250 °C, the melt amount increases from 35 to 43 %, so to obtain products with a maximum sintering degree, it is necessary to conduct firing at a temperature not lower than 1,200 °C. It was found that in a temperature range of 1,100–1,250 °C the melt viscosity of mass P-1 decreases (from $10^{4.76}$ Pa·s to $10^{4.29}$ Pa·s), surface tension increases (from 0.275 to 0.285 mN/min) and the melting activity decreases (from 0.1146 to 0.1078 rel. units) due to melting saturation with Al_2O_3 and SiO_2 oxides. In the same temperature range, the melt viscosity of mass P-2 decreases (from $10^{4.83}$ to $10^{4.47}$ Pa·s), and the melting activity decreases significantly (from 0.1578 to 0.1179 rel. units) with unchanged surface tension (0.290 mN/m). The data obtained made it possible to identify a rational area for the use of the new composition and to determine the optimal product firing temperature before conducting experimental studies. Subsequently, composition P-1 was used to obtain porcelain tiles with a firing temperature

of 1,150 °C. Composition P-2 became the basis for the development of electrical porcelain with a firing temperature of 1,200 °C.
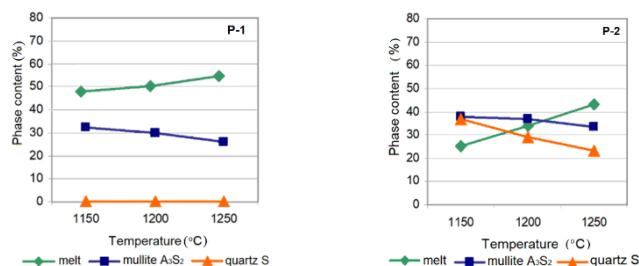

Figure 2: The phase formation dynamics during firing of masses in the temperature range of 1,150-1,250 °C

The experimental verification of the calculations results made it possible to formulate the following principles for mass compositions design on the base $Na_2O–K_2O–Al_2O_3–SiO_2$ system for obtaining various purposes fineceramic products with a temperature formation of 1150–1200 °C:

1) The design of the composition of long-term firing products should be carried out in the central part of the NAS_6-KAS_6-A_3S_2-S tetrahedron. This provides a large amount of highly active melt formation during firing with a viscosity of $10^{3.7}$–$10^{4.7}$ Pa·s and a surface tension of up to 0.3 mN/m. It is crystallisation capable, increasing the product's operational properties.

2) For products of high-speed firing, the choice of the composition should carry out in the region of the NAS_6-KAS_6-A_3S_2-S tetrahedron adjacent to the KAS_6-NaS_6-S edge. To ensure intensive liquid-phase sintering without the risk of product high-temperature deformation, the viscosity and surface tension of the highly active melt formed during firing should be at the level of $\eta=10^{3.0}$–$10^{3.7}$ Pa·s; $\delta \leq 0.3$ mN/m.

3) In the production of porcelain tiles and products household, sanitary, and electrical porcelain, effective energy costs reducing means is the use of non-fritt glass-cristal glazes. This approach makes it possible to exclude fritting as one of the most energy-consuming technological stages. When designing glazes, one should choose compositions that form a rapid crystallisation melt capable and having at a given firing temperature low viscosity ($\eta=10^{2.5}$–$10^{3.0}$ Pa·s) and a surface tension $\delta \leq 0.3$ mN/m.

4. Industrial implementation

The experience gained in many years of research results in the industrial production of fine-ceramic products for various functional purposes. It testifies the effectiveness of the considered technological principles used for the energy-saving implementation in the production of porcelain tiles (Rychchenko et al., 2008), table wares (Fedorenko et al., 2013), sanitary and electrical porcelain (Rychchenko et al., 2009). The use of developed non-fritted glazes makes it possible to exclude the highly energy-intensive operation of fritting from the production technological cycle. Wares properties are presented in Table 1.

Table 1: Characteristics of developed ceramic materials

Firing parameters and product properties	Porcelain tiles	Porcelain tableware	Sanitary-porcelain	Electro-porcelain
Firing temperature, °C	1,150	1,150	1,180	1,200
Firing temperature decreasing, °C	50	150	100	150
Reduction in firing time, %	17	17	15	12
Water absorption, %	0,3	0,1	0,2	0
Bending strength, MPa	42	55	58	63
Tensile strength, MPa	–	–	–	31
Wear resistance, mm^3	150	–	–	–
Whiteness, %	65	78 (84*)	72 (80*)	–
CLTE $\alpha \cdot 10^6$, 1/°C	5,8	5,6	5,4	4,9
Resistivity ρ_V, Ohm·cm (f = 50 Hz)	–	–	–	$4,1 \cdot 10^{14}$
Breakdown voltage kV·mm^{-1} (f = 50 Hz)	–	–	–	30
Compliance to Standard	ISO 13006 (group B1a)	ISO/DIS 5644	EN 14411	IEC-60672-3 Group C110

* properties of glazed products

5. Conclusions

Carrying out a complex of theoretical and experimental studies made it possible to set the principles of designing compositions of ceramic masses and glazes for long-term and high-speed energy-saving firing. It is based on graph-analytical studies in systems of phase-forming oxides. The advantage of this approach is the predicting possibility of the melt characteristics for given firing conditions of products, which makes it possible to determine preliminarily (before the experiment) the temperature which ensures the maximum degree of material sintering. It ensures preventing of high-temperature deformation of products due to the monitoring of the dynamics of liquid phase accumulation and also to influence their properties by controlling the processes of phase formation in conditions of energy-saving firing. The obtained methodology has been tested successfully and implemented at Ukrainian enterprises producing porcelain tiles and porcelain products for various purposes. Feasibility studies confirmed the efficiency of using the developed materials. Implementation of these developments allows to obtain products with a complex of high-performance characteristics and a reduction of natural gas consumption by 25-30 % due to a temperature decrease by 50-150 °C and a reduction of the firing duration by 12-17 %.

References

Almeida M.I., Dias A. C., Demertzi M., Arroja L., 2016, Environmental profile of ceramic tiles and their potential for improvement. Journal of Cleaner Production, 131, 583-593, DOI:10.1016/j.jclepro.2016.04.131.

Caglayan H., Caliskan H., 2019, Thermo-ecological analysis of industrial kilns. Journal of Environmental Management, 241, 149-155, DOI: 10.1016/j.jenvman.2019.04.032.

Castro Oliveira M.; Iten M.; Cruz P.L.; Monteiro H., 2020, Review on Energy Efficiency Progresses, Technologies and Strategies in the Ceramic Sector Focusing on Waste Heat Recovery, Energies, 13, 6096, DOI:10.3390/en13226096.

Cuviella-Suárez C., Colmenar-Santos A., Borge-Diez D., Rosales-Asensio E., 2019, Sanitary-ware factories: heat recovery strategies to optimize energy and water consumption, Energy Procedia, 157, 719-736, DOI:10.1016/j.egypro.2018.11.238.

Delpech B., Milani M., Montorsi L., Boscardin D., Chauhan A., Almahmoud S., Axcell B., Jouhara H., 2018, Energy efficiency enhancement and waste heat recovery in industrial processes by means of the heat pipe technology: Case of the ceramic industry, Energy, 158, 656-665, DOI:10.1016/j.energy.2018.06.041.

Fedorenko E.Y., Ryshchenko M.I., Daineko E.B., Chirkina M.A., 2013, Energy-saving technology for household porcelain, Glass and Ceramics, 70, 219-222.

Ferrer S., Mezquita A., Aguilella V.M., Monfort E., 2019, Beyond the energy balance: Exergy analysis of an industrial roller kiln firing porcelain tiles. Applied Thermal Engineering, 150, 1002-1015, DOI:10.1016/j.applthermaleng.2019.01.052.

Flugel A., 2007, Glass viscosity calculation based on a global statistical modeling approach. Glass Technology: Eur. J. Glass Science and Technology, Part A, 48, 13–30.

Giacone E., Mancò S., 2012, Energy efficiency measurement in industrial processes. Energy, 38, 1, 331-345. DOI:10.1016/j.energy.2011.11.054.

Goleus V.I., Saley A.A., 2015, The calculation of the viscosity of molten borosilicate enamels as a function of their composition and temperature. Issues of Chemistry and Chemical Technology, 1, 44-47 (in Russian).

Kapustenko P., Klemeš J.J., Arsenyeva O., Fedorenko O., Kusakov S., Bukhkalo S., 2020, The Utilisation of Waste Heat from Exhaust Gases after Drying Process in Plate Heat Exchanger. Chemical Engineering Transactions, 81, 589-594, DOI:10.3303/CET2081099.

Mezquita A., Boix J., Monfort E., Mallol G., 2014, Energy saving in ceramic tile kilns: Cooling gas heat recovery. Applied Thermal Engineering, 65, 1–2, 102-110, DOI: 10.1016/j.applthermaleng.2014.01.002.

Monfort E., Mezquita A., Granel R., Vaquer E., Escrig A., Miralles A., Zaera V., 2010, Analysis of energy consumption and carbon dioxide emissions in ceramic tile manufacture, Bulletin de la Sociedad Espanola de Ceramica y Vidrio, 49(4), 303-310 (in Spanish).

Mullinger P., Jenkins B., 2022, Industrial and Process Furnaces: Principles, Design and Operation, Butterworth-Heinemann (Copyright Elsevier Ltd.), 363-400, DOI: 10.1016/C2020-0-04546-9.

Rychchenko M.I., Shchukina L.P., Fedorenko E.Y., Firsov K.N., 2008, Possibility of obtaining ceramogranite using quartz-feldspar raw material from Ukraine, Glass and Ceramic, 65, 1–2, 23 –26.

Ryshchenko M.I., Fedorenko E.Yu., Chirkina M.A., Karyakina É.L., Zozulya S.A., 2009, Microstructure and properties of lower-temperature porcelain, Glass and Ceramics, 66, 11-12, 393–396.

Song B., 2018 The research on energy-saving reconstruction of ceramic kiln based on engineering system theory. Chemical Engineering Transactions, 66, 601-606, DOI:10.3303/CET1866101.